Electronic Supplementary Material (ESI) for Journal of Materials Chemistry A.
This journal is © The Royal Society of Chemistry 2018

Supplementary Information

Plasmon-Engineered Anti-Replacement Synthesis of Naked Cu Nanoclusters with Ultrahigh Electrocatalytic Activity

Shusheng Pan[1*], Xian Zhang[2,3,4], Wei Lu[5], Siu Fung Yu[5,6*]

[1] *Department of Physics, School of Physics and Electrical Engineering, Guangzhou University, Guangzhou 510006, People's Republic of China*

[2] *Key Laboratory of Materials Physics, Anhui Key Laboratory of Nanomaterials and Nanostructures, Institute of Solid State Physics, Hefei Institutes of Physical Science, Chinese Academy of Sciences, Hefei 230031, People's Republic of China*

[3] *Centre for Environmental and Energy Nanomaterials, CAS Center for Excellence in Nanoscience, Chinese Academy of Sciences, Hefei 230031, China*

[4] *University of Science and Technology of China, Hefei 230026, China*

[5] *Department of Applied Physics, The Hong Kong Polytechnic University, Hung Hom, Kowloon, Hong Kong*

[6] *Shenzhen Research Institute, The Hong Kong Polytechnic University, Shenzhen PR China*

[*]Corresponding authors: Prof. Pan, sspan@gzhu.edu.cn; Prof. Yu, sfyu21@hotmail.com

Experimental details:

1. **Fabrication of Au nanoparticles colloidal solutions:** High purity (99.99%) Au plate ($1\times0.6\times0.1cm^3$) was perpendicularly placed at the bottom of a glass bottle containing 10~30 mL DI water (conductivity: 1μs/cm). The Au plate was irradiated by a pulsed laser beam (6 ns, 10 Hz) with wavelength of 1064 nm and a peak density of 150 MW/cm^2, see figure S1(a) After the Au plate ablating for 10~30 min, the DI water appeared to be pink in color. This indicated that the formation of Au nanoparticles. The Au nanoparticles have spherical shape with average diameter of ~ 10-20 nm. The concentration of Au nanoparticles solution is determined from the mass loss of Au plates before and after laser ablation.

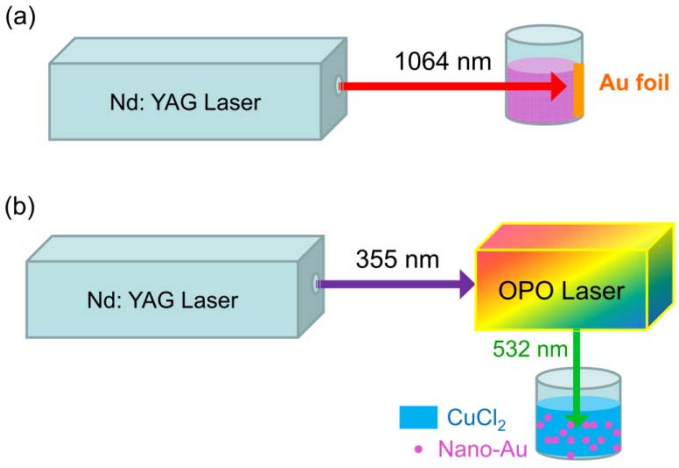

Figure S1(a) Fabrication of Au nanoparticles by pulsed laser ablation of Au plate in water, and (b) photochemical reaction between Au nanoparticles and $CuCl_2$ under 532 nm pulsed laser illumination.

2. The anti-replacement reaction by laser irradiation: The 3~10 mL $CuCl_2$ (Sigma, purity: 99.99%, concentration: 0.1~40 mg/mL) and 2~10 mL colloidal pulsed laser ablation-Au solution (concentration: 0.01~0.1 mg/mL) were mixed together and stirred for 5~20 minutes in dark room. The intermixture of Au nanoparticles and $CuCl_2$ were then irradiated by 532 nm pulsed laser (6 ns, 10 Hz, Gauss beam diameter of 0.5 cm) generated from a frequency doubled Nd:YAG laser (Continuum Powerlite DLS 9010), see figure S1(b).The laser peak power density is 10^6~10^7 W/cm^2. The irradiation duration is 1~10 minutes. Furthermore, the intermixture of Au nanoparticles and $CuCl_2$ were irradiated by pulsed laser beam (6 ns, 10 Hz, Gauss beam diameter of 0.5 cm) of different wavelengths (440 nm, 506 nm, 540 nm, 600 nm,

720 nm and 815 nm) generated from the optical parametric oscillator (OPO, Continuum Panther EX) under excitation from by a 355 nm laser beam generated by the frequency tripled Nd:YAG pulsed laser. The laser power and irradiation duration were set to 3×10^5 W/cm^2 and 5 seconds, respectively. After the reaction takes place, centrifugation (10,000~12,000 rpm, 15 min) and cleaning by water were applied to separate the Cu nanoclusters from the residual solution. The obtained Cu nanoclusters sediments were ultrasonically dispersed in water or ethanol. The zeta potential of Cu nanoclusters in water is about -12 mV.

3. **Characterization:** Cu nanoclusters were loaded on a carbon-coated molybdenum grid. High resolution transmission electron microscopy (HRTEM) was performed using a JEM-2100F transmission electron microscope (TEM) with an accelerating voltage of 200 kV. X-ray photoelectron spectroscopy (XPS) (ESCALAB 250, Thermo-VG Scientific, Al Kα, pass energy: 30 eV) was used to characterize the chemical states with adventitious C 1s calibration peak of 284.8 eV. The concentrations of Au ions in solution after 12,000 rpm centrifugation were measured by an inductively coupled plasma atomic emission spectrophotometer (ICP, model: ICP-6300, Thermo Fisher, USA).

4. **Optical absorption and photoluminescence:** The UV-vis absorption spectrum of the Au and Cu nanoclusters in water was measured by using a SHIMADZU UV-3600 spectrometer. The steady photoluminescence spectra were collected by Horiba Jobin YvonFluorolog-3 with 450 W xenon lamp as excitation light. The time-resolved photoluminescence spectrum was collected by IBH-TEMPRO-01 (Horiba JobinYvon) under the excitation of 350 nm nano-LED.

5. Electrochemical characterization:A glassy carbon (GC) disk electrode (5.0 mm in diameter) was first polished with 5.0, 3.0 and 0.05μm alumina slurry sequentially and then washed ultrasonically in the mixture of water and ethanol for 40 s. The cleaned electrode was dried under N_2 gas ambient. The catalyst was prepared by ultrasonically the dispersing Cu nanoclusters into a mixture including 20 μL Nafion solution (0.5wt%) and 80 μL ethanol. And 10 μL catalyst ink was casted onto the GC electrode surface with loading amount of 0.2μg of Cu nanoclusters. Electrochemical characterization were carried out on an electrochemical

workstation (CHI 760D,CH Instruments, Inc., Shanghai, China) coupled with a PINE rotating disk electrode (RDE) system (Pine Instruments Co. Ltd. USA). A standard three-electrode (GC working electrode, Ag/AgCl reference electrode, and platinum wire counter electrode) electrochemical cell equipped with gas flow system was employed during measurements.

According to the TEM, EDS and XPS characterization, all the Au nanoparticles are transformed to Au^{3+} and Au^{+} ions in the solution after laser irradiation. The concentration of Au nanoparticles is 0.01 mg/mL determined from the weight loss of Au plate before and after laser ablation. Based on the proposed reaction process $Au + Cu^{2+} \rightarrow \frac{1}{2}Au^{3+} + \frac{1}{2}Au^{+} + Cu$,the as-prepared Cu nanoclusters sediments is estimated to 0.006 mg. The concentration of Cu nanoclusters dispersed in 0.3 mL ethanol is 0.02μg/μL. The value is well consistent with the ICP results (~18 ppm) through dissolving the Cu nanoclusters into the solution containing the mixture of HNO_3 and HCl.

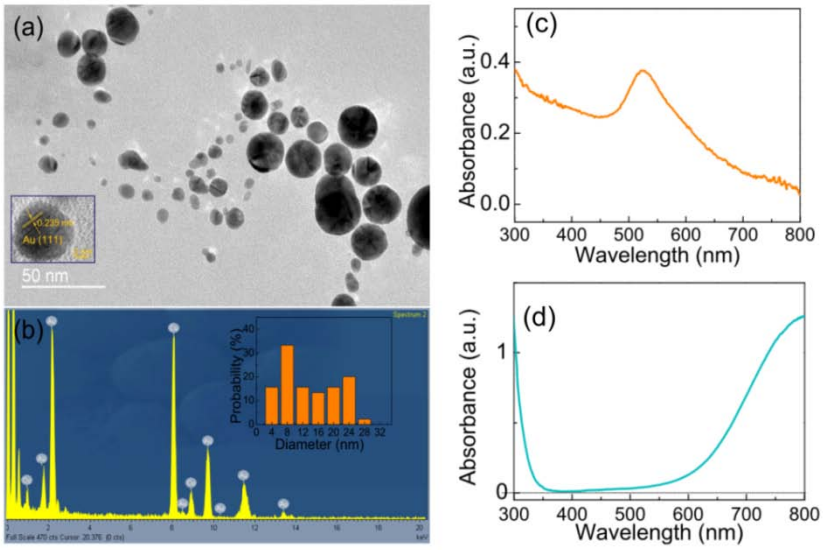

Figure S2.(a) TEM image, inset, high resolution transmission electron microscopy (HRTEM) of Au nanoparticles; (b) energy dispersion spectroscopy (EDS) result of Au nanoparticles, inset Au particles size distribution; optical absorption of Au nanoparticles (c), and $CuCl_2$ solutions (d).The Au nanoparticles are sphere-like with average diameter of10-20 nm. Clear lattice stripe with distance of 0.235 nm corresponding to Au (111) plane can be observed in the HRTEM.

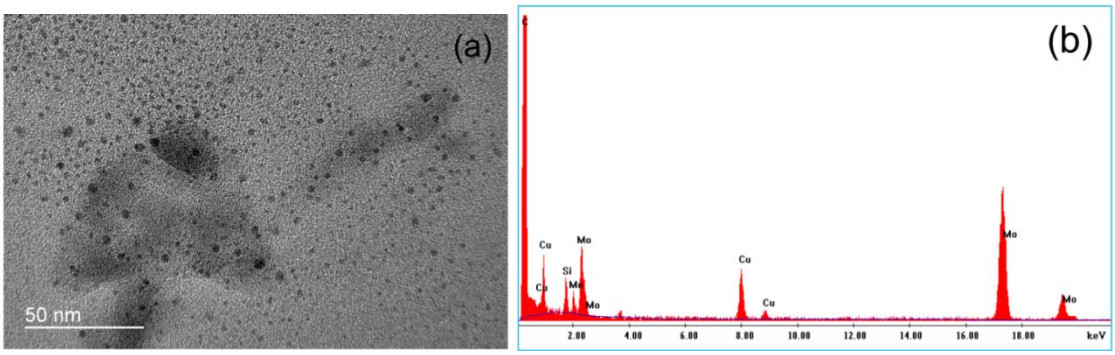

Figure S3.(a) TEM image, and (b) EDS results of Cu nanoclusters probed at another spot. The Si signal originates from the detector, Mo and C from the supported grid.

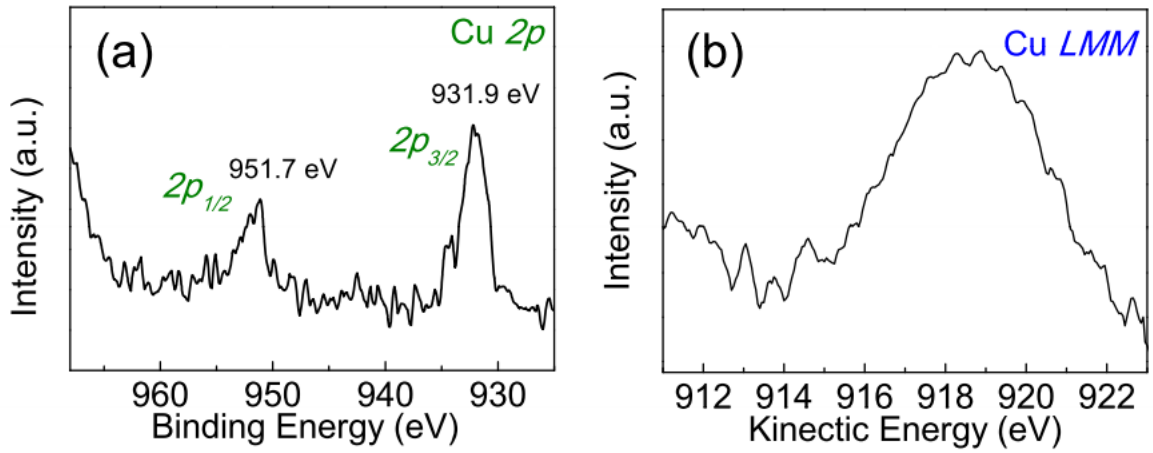

Figure S4.(a) Cu 2p XPS probed from the Cu nanoclusters sediments at different spot, (b) Cu LMMX-ray excited Auger Electron Spectroscopy spectrum of Cu nanoclusters.

No obvious shakeup satellite peaks can be observed, as shown in Figure S4. The Cu 2p binding energy is well consistent with the reported values of Cu (0).[R1,2] The Cu $L_3M_{45}M_{45}$ Auger electron peaks at ~ 919 eV are characteristic of metallic Cu.[R3]

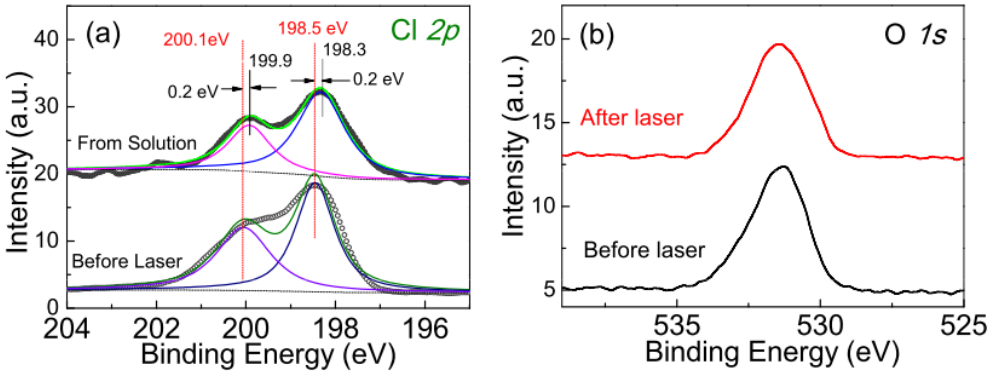

Figure S5. The high resolution X-ray photoelectron spectroscopy (a) Cl 2p, (b) O1s. Curve "before laser" in (a) and (b) refers to the corresponding spectra recorded from the mixture of $CuCl_2$ and Au nanoparticles, curve "from solution" in (a) refers to the dried sample from the resultant solution after chemical reaction under laser irradiation, curve "after laser" in (b) refers to the O from the Cu nanoclusters sediments.

The Cl $2p_{3/2}$ binding energy from solution is 0.2 eV lower than that from $CuCl_2$, as shown in Figure S5(a).The reported Cl $2p_{3/2}$ binding energy in AuCl and $CuCl_2$ is 198.2 eV[R4]and 198.5 eV[R5](after calibration modifying), respectively. The Cl 2p from solution can be assigned to be originated from a mixture of unreacted $CuCl_2$ and generated gold chloride-related compounds.

The O 1s binding energy located at 531.5 eV from Cu nanoclusters can be attributed to adsorbed organic C-O compound bonding, which is same to the sample (mixture of $CuCl_2$ and Au nanoparticles) before reaction.

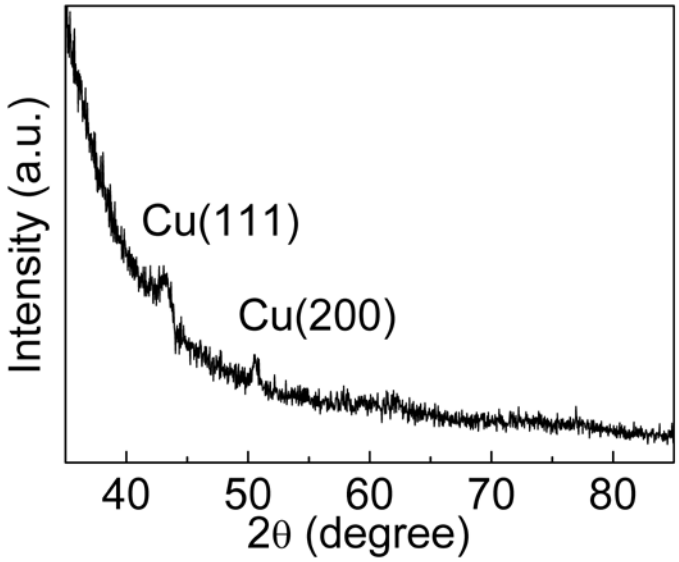

Figure S6. Grazing angle XRD pattern of Cu nanoclusters on Si wafer

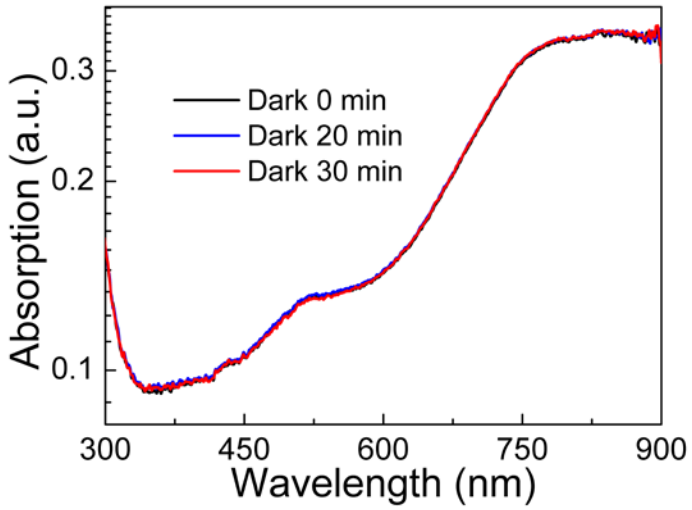

Figure S7. Absorption spectrum of intermixture of $CuCl_2$ and Au stored in dark room with different time interval.

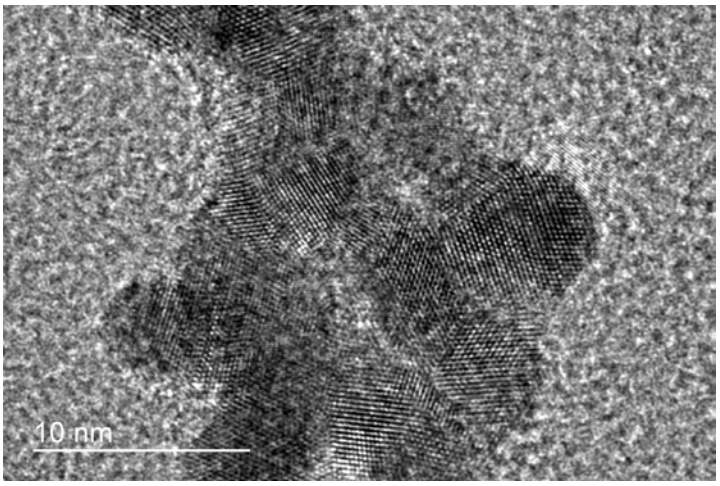

Figure S8. HRTEM of Cu nanoclusters scrapped from the electrode after the electrolysis measurement.

The nanoclusters are agglomeration after electrolysis, as shown in Figure S8. We attributed the decrease of the reduction current to the lower surface active area of nanoclusters caused by agglomeration.

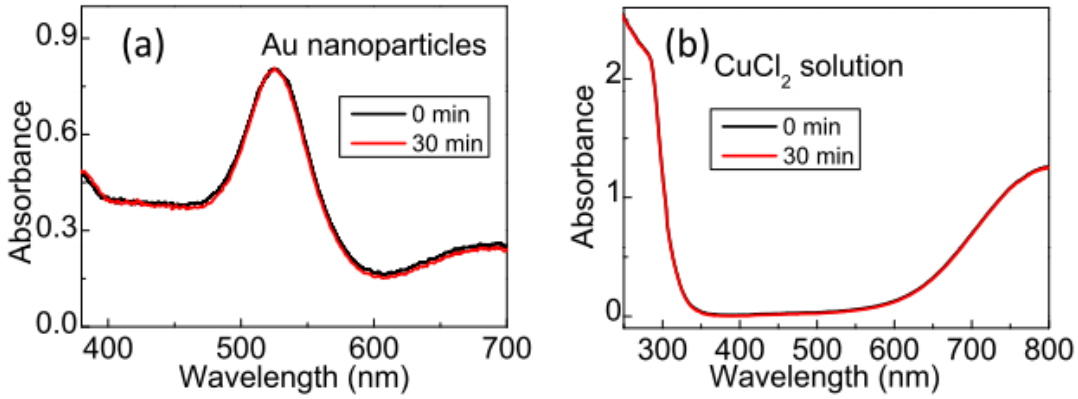

Figure S9. Optical absorption spectrum of Au nanoparticles and $CuCl_2$ solution irradiated by 532 nm laser with peak power density is 10^6 W/cm^2.

Table S1. Au 4f XPS peaks fitted results of Au nanoparticles and samples from residual solution after anti-replacement reaction under laser irradiation.

	Binding Energy (eV)		FWHM (eV)		Assignment
	Au nanoparticles	residual solution	Au nanoparticles	residual solution	
Au 4f5/2		89.8		0.8	Au^{3+}
		88.5		0.9	Au^{+}
	87.9		0.9		Au
Au 4f7/2		86.1		1.6	Au^{3+}
		84.8		1.9	Au^{+}
	84.2		1.2		Au
Au 4f spin orbit split		3.7 eV for Au (0) in Au nanoparticles 3.7 eV (both Au (III) and Au (I)) in residual solution			

Table S2. PL decay curve Fitted parameters for Cu nanoclusters

τ_1 *(Instrument Response)*	τ_2	A_1	A_2	CHISQ
0.81 ns	**15.6ns**	**0.122**	**0.00241**	**0.751**

PL decay profiles were fitted by two exponential function equation: $I(t) = t_0 + A_1 * \exp(-t/\tau_1) + A_2 * \exp(-t/\tau_2)$. τ_1 and τ_2 denote the decay time for the faster and the slower components, and A_1 and A_2 are the PL amplitudes.

Table S3. Comparison of reduction current of metal nanoclusters

Materials	Loading Weight	Reduction Current Density per Weight @ -0.9V	Size	Ref.
$Au_{140}(S(CH_2)_5CH_3)_{53}$	10μg	170 mA/(cm^2·mg)	1.7 nm	R6
$Cu_{12}DT_8Ac_4$	50 μg	2.5 mA/(cm^2·mg)	2.0 nm	R7
$Cu_8(C_7H_9N_2S)_4$	10 μg	57 mA/(cm^2·mg)	—	R8
Cu	0.2 μg	3750 mA/(cm^2·mg)	2.0 nm	This work

Reference:

R1. Juntunen, M. A., Heinonen, J., Vähänissi, V., Repo, P., Valluru, D. & Savin, H. Near-unity quantum efficiency of broadband black silicon photodiodes with an induced junction. *Nat. Photonics***10**, 777-781, (2016).

R2. Saran, R. & Curry, R. J. Lead sulphide nanocrystal photodetector technologies. *Nat. Photonics***10**, 81-92, (2016).

R3. Schön, G. ESCA studies of Cu, Cu2O and CuO. *Surface Science***35**, 96-108, (1973).

R4. Kishi, K. & Ikeda, S. X-ray photoelectron spectroscopic study of the reaction of evaporated metal films with chlorine gas. *The Journal of Physical Chemistry***78**, 107-112, (1974).

R5. Sesselmann, W. & Chuang, T. J. The interaction of chlorine with copper: I. Adsorption and surface reaction. *Surface Science***176**, 32-66, (1986).

R6. Chen, W. & Chen, S. Oxygen Electroreduction Catalyzed by Gold Nanoclusters: Strong Core Size Effects. *Angewandte Chemie International Edition***48**, 4386-4389, (2009).

R7. Wu, Z., Li, Y., Liu, J., Lu, Z., Zhang, H. & Yang, B. Colloidal Self-Assembly of Catalytic Copper Nanoclusters into Ultrathin Ribbons. *Angewandte Chemie International Edition***53**, 12196-12200, (2014).

R8. Salorinne, K., Chen, X., Troff, R. W., Nissinen, M. & Hakkinen, H. One-pot synthesis and characterization of subnanometre-size benzotriazolate protected copper clusters. *Nanoscale***4**, 4095-4098, (2012).